University of Illinois at Urbana-Champaign

Term Project
MATSE385/PHYS363 – Atomic Scale Simulations
Fall Semester 2001

Thermostats, Pressure Controls

and the simulation of homogeneous nucleation

Paul Erhart
Department of Materials
Science and Engineering

Jan Kretzschmar
Department of
Physics

Abstract

The Verlet integrator as well as the Nosé-Hoover thermostat and pressure control have been implemented into an existing molecular dynamics simulation.

The homogeneous nucleation from the vapor phase has been studied for copper.

Contents

1 Introduction

Most experiments are carried out under conditions of constant temperature and pressure. On the other hand, standard molecular dynamics (MD) simulations integrate the Newtonian equations of motion in an MD cell of fixed volume, V. The conserved quantity is the total energy E. Assuming particle conservation these situations are described by the microcanonical (N,V,E), canonical (N,V,T), isobaric-isenthalpic (N,P,H) and isobaric-isothermal (N,P,T) ensembles.

Using fundamental statistical mechanics one can show that the averages obtained from canonical and microcanonical ensembles differ by a factor of the order of $1/\sqrt{N}$. In the case of macroscopic systems one can neglect this difference and it indeed vanishes at the thermodynamic limit. Nevertheless one has to keep in mind this result is strictly valid for systems at equilibrium.

The systems which can be investigated by typical MD simulations are way smaller than real ones. In our particular case the system contains about 600 particles. From the relation mentioned above the averages computed in the microcanonical and the canonical ensembles should differ by approximately four per cent.

The objective of this project is to study nucleation from the vapor phase in metallic systems. In experiments rare gases are used to cool down the system. This is to be compared with the techniques to control the kinetic energy – that is to set the temperature – available for MD simulations. In the next section we will discuss the theory and implementation of several approaches developed throughout the last twenty years as well as compare and illustrate their aptitude to sample the various ensembles. Due to the existing structure of the code used we give an short overview in chap. 4 of the two integration schemes involved, namely the Gear predictor-corrector algorithm and the Verlet integrator. Afterwards the calculation of energies and forces with the EAM and Lennard-Jones potentials is surveyed. The configuration of our simulations is described in section chap. 6. chap. 7 summarizes the results and their interpretation. Finally we will discuss the deficiencies of our approach and possible improvements.

2 Thermostats

2.1 Theory

As outlined previously there is a considerable interest in methods to sample the canonical distribution with MD simulations and various techniques have been invented.

In the case of the canonical (N,V,T) ensemble the instantaneous kinetic energy is the conserved quantity in place of the total energy in the case of the microcanonical (N,V,E) ensemble. The most simple method to realize this situation in a simulation is by scaling the velocities. But one cannot expect to sample thereby the canonical ensemble. The same is true for two other techniques, the first one (Andersen, 1980) employs random forces, the second one (Berendsen et al., 1984) is a more subtle way to scale the velocities. The scaling factor χ of the Berendsen thermostat is given by (Allen and Tildesley, 1989)

$$\chi = \left(1 + \frac{\delta t}{\tau}\left(\frac{T}{\mathcal{T}} - 1\right)\right)^{1/2} .$$

Here T is the desired temperature, $\mathcal{T}$ the instantaneous kinetic temperature, δt the time step and τ represents a rate which determines the coupling to the system.

Nosé was the first to come up with a proper modification of the equations of motion so that they reproduce the canonical ensemble (Nosé, 1984). He introduces another degree of freedom s which acts as a scaling factor for the velocities (or the time step, equivalently). Due to the parameter additional terms associated with its potential and kinetic energy appear in the Lagrangian and Hamiltonian, respectively. The conserved quantities in this system are the Hamiltonian, the total momentum and the total angular momentum. The equations of motion as derived from the Hamiltonian

$$\mathcal{H}_{\text{Nosé}} = \sum_i \frac{\mathbf{p}_i^2}{2m_i s^2} + \phi(\mathbf{r}) + \frac{p_s^2}{2Q} + (f+1)kT_{eq} \ln s$$

are

$$\begin{aligned} \ddot{\mathbf{r}}_i &= -\frac{\mathbf{F}_i}{m_i s^2} - \frac{2\dot{s}}{s}\mathbf{r}_i \\ Q\ddot{s} &= \sum_i m_i s \ddot{\mathbf{r}}_i^2 - \frac{(f+1)kT_{eq}}{s} \end{aligned}$$

where $\mathbf{p}_i$ are the momenta of the particles, $\mathbf{r}_i$ their positions and $\mathbf{F}_i$ the forces acting on them. f stands for the number of degree of freedom of the unbiased system, p_s is the conjugated momentum of s and the parameter Q determines the coupling of the system to the *heat bath*: the smaller it is the stronger the coupling. These equations are smooth, deterministic and on the contrary to the prementioned methods time-reversible. In fact, this approach represents a microcanonical ensemble with an additional coordinate. Using Liouville's theorem it can be shown that it is equivalent to a canonical ensemble with f degrees of freedom.

Nosé's equations were reformulated (Hoover, 1985) avoiding the scaling of the time step by introducing a new timestep containing s. Furthermore Hoover defined a friction coefficient $\xi \equiv p_s/Q$. The equations of motion become

$$\left.\begin{array}{rcl} \ddot{\mathbf{r}}_i &=& \frac{\mathbf{F}_i}{m} - \xi \dot{\mathbf{p}}_i/m_i \\ \dot{\xi} &=& Q^{-1}\left(\sum_i \mathbf{p}_i^2/m_i - (f+1)kT_{eq}\right) \end{array}\right\} \tag{1}$$

Posch showed the effectiveness of the Nosé thermostat in sampling phase space for the classical one-dimensional harmonic oscillator (Posch et al., 1986). Plotting p versus q for the microcanonical ensemble a perfect circle is obtained. Andersens method generates a number of points scattered over a circle. The Nosé-Hoover thermostat gives a broadened circle as expected if one allows fluctuations in the total energy (noting that the phase space volume corresponds to energy).

2.2 Implementation

In order to solve the eqs. (1) computationally they have to be discretized. Resolving the finite difference equations allows their implementation into the code. Holian gave explicit formulations for the Verlet algorithm (Holian et al., 1990) which translate to code as follows.

```
! x0,x1,x2 = positions and time derivatives in scaled units
real*8,dimension(3*NPMAX) :: x0,x1,x2
! f        = forces
real*8,dimension(3*NPMAX) :: f
! xi       = friction coefficient
real*8 :: xi
! trans    = kinetic energy in units of kB
real*8 :: trans
x2(i) = x2(i) - f(i)*x1(i)
x0(i) = two*x0(i) - x0old(i) + x2(i)
transavg = half*(trans+transold)
transold = trans
dK = two/(three*temp)*transavg - one
xi(i) = xi(i) + four*dK*deltat_fs/Q
```

In fig. 1 the temperature as a function of time as obtained in the MD simulation is shown. The cubic simulation box with side length 36.15 Åcontained 2000 Cu atoms arranged on an fcc lattice. The initial velocities were set according to the Maxwell-Boltzmann distribution at temperature 600 K.

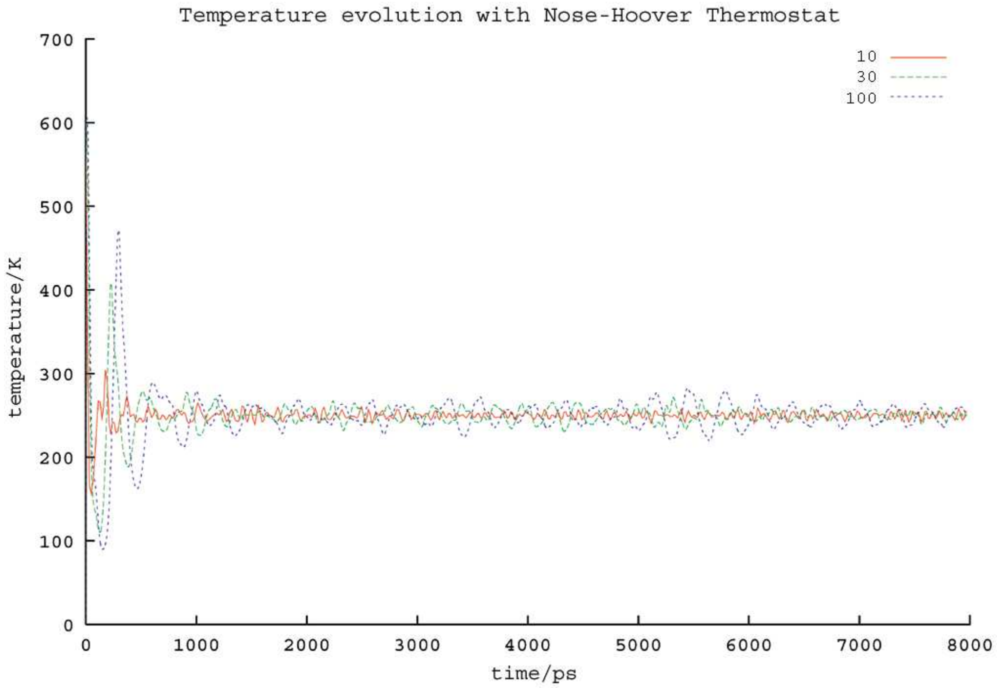

Figure 1: The evolution of temperature with time for the Nosé-Hoover thermostat for different values of the coupling constant Q

Nosé has also given an expression for the period of oscillation depending on the choice of Q:

$$t_0 = 2\pi \left(\frac{Q \langle s \rangle^2}{2fkT_{eq}} \right)^{1/2}$$

Another way to check if the thermostat operates correctly is to compute the heat capacity from the energy fluctuations

$$\langle \Delta E^2 \rangle_{NVT} = \langle E^2 \rangle_{NVT} - \langle E \rangle_{NVT}^2 = kT^2 C_V$$

which can be rewritten in terms of the temperature and the fluctuations of the temperature

$$\langle \Delta T^2 \rangle_{NVE} = T_{eq}^2 \frac{2}{3N} \left(1 - \frac{3}{2C_V} \right).$$

3 Pressure controls

3.1 Theory

The development of pressure controls is similar to those of the thermostats. However the pressure controls do not only alter the motion of the particles by modifying either the velocities or the accelerations but also vary the box size.

The first approach (Andersen, 1980) used volume scaling exclusively. A method analogous to the Berendsen thermostat has been devised where the system is coupled to a *pressure bath* (Berendsen et al., 1984). The instantaneous pressure P has to obey the equation (Allen and Tildesley, 1989)

$$\dot{P} = (P_{ext} - P)/t_P$$

while the volume is scaled by a factor χ given by

$$\chi = 1 - \frac{\delta t}{t'_P}(P_{ext} - P).$$

P_{ext} is the desired pressure, t_P, t'_P are time constants and δt is the time step. As in the case of the temperature control this does not sample the isobaric-isenthalpic ensemble.

Nosé accomplished this task again by introducing an additional degree of freedom. In the general case not only the volume is allowed to change but also the shape of the cell (Nosé and Klein, 1983; Parrinello and Rahman, 1980). One can also include the rotational degree of freedom for molecules but here we are interested in monatomic systems only. Additionally we restrict ourselves to cubic cells. The *real* coordinates $\mathbf{r}$ are scaled with respect to the volume V, i.e. $\mathbf{r}_i = V^{1/3}\mathbf{x}_i$ The corresponding Hamiltonian becomes

$$\mathcal{H} = \sum_i \frac{\mathbf{p}_i^2}{2m_i s^2 V^{2/3}} + \phi(V^{1/3}\mathbf{x}) + \frac{W\dot{V}^2}{2} - P_{ext}V \tag{2}$$

from which the equations of motion can be obtained in the usual way. The coupling between the system and the pressure control is adjusted by the parameter W.

As it has been pointed out (Hoover, 1986) one is free to choose a pair of variables from the set V-$\dot{V}$-$\dot{\varepsilon}$-$\ddot{\varepsilon}$ where V denotes the volume $\dot{\varepsilon}$ the strain rate and $\dot{V}$, $\ddot{\varepsilon}$ the corresponding time derivatives. Specifically to describe the evolution of volume with time either $\dot{V}$ (Nosé and Andersen) or $\dot{\varepsilon}$ can be used. Hoover decided to take the latter one. Again using the transformations to eliminate the scaling parameter described above s he ended up with the following set of equations:

$$\left.\begin{array}{rcl} \ddot{\mathbf{x}} & = & \frac{\mathbf{F}_i}{m_i s^2 V^{1/3}} - \frac{2}{3}\frac{\dot{V}}{V}\dot{\mathbf{x}}_i \\ \dot{V} & = & 3V\dot{\varepsilon} \\ \ddot{\varepsilon} & = & (P - P_{ext})V/kT\tau^2 \end{array}\right\} \tag{3}$$

τ determines the coupling of the system to the pressure control. It can be interpreted as the relaxation time of the hypothetical 'piston' exerting the external pressure. $\mathbf{x}_i$ are the scaled coordinates introduced earlier.

Now we are in the position to combine the Nosé-Hoover thermostat and pressure control to end up with a formulation that allows simulations in the isobaric-isothermal ensemble.

3.2 Implementation

Applying finite differences permits us to implement eqs. (3) (Holian et al., 1990).

A possibility to test the pressure control is provided by the calculation of the bulk modulus (Nosé and Klein, 1983). This method is equivalent to the computation of the heat capacity described as a check for the thermostat.

$$B_s = -V\left(\frac{\partial P}{\partial V}\right)_s = \frac{VkT}{\langle(\delta V)^2\rangle}$$

In fig. 2 the pressure as a function of time as obtained in the MD simulation is shown. One sees the effects of the coupling constant.

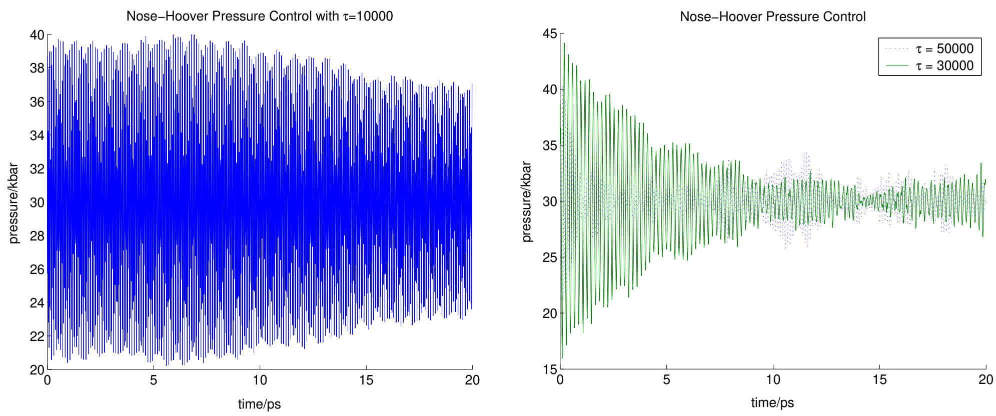

Figure 2: The evolution of pressure with time for the Nosé-Hoover control for different values of the coupling constant τ, left graph shows example for too weak coupling

4 Integration of the equations of motion

4.1 Gear predictor-corrector algorithm

The existing code provided an implementation of the sixth order Gear predictor-corrector algorithm. The Berendsen thermostat and pressure control modulate the evolution of the system by scaling the velocities.

Defining scaled time derivatives of $\mathbf{r} = \mathbf{r}_0$ as $\mathbf{r}_1 = \delta t(\mathrm{d}\mathbf{r}_0/\mathrm{d}t)$, $\mathbf{r}_2 = \frac{1}{2}\delta t^2(\mathrm{d}^2\mathbf{r}_0/\mathrm{d}t^2)$, $\mathbf{r}_3 = \frac{1}{6}\delta t^3(\mathrm{d}^3\mathbf{r}_0/\mathrm{d}t^3)$, etc., the predictor step for a fourth order Gear algorithm can be written in matrix form (Allen and Tildesley, 1989)

$$\begin{pmatrix} \mathbf{r}_0^p(t+\delta t) \\ \mathbf{r}_1^p(t+\delta t) \\ \mathbf{r}_2^p(t+\delta t) \\ \mathbf{r}_3^p(t+\delta t) \end{pmatrix} = \begin{pmatrix} 1 & 1 & 1 & 1 \\ 0 & 1 & 2 & 3 \\ 0 & 0 & 1 & 3 \\ 0 & 0 & 0 & 1 \end{pmatrix} \begin{pmatrix} \mathbf{r}_0(t) \\ \mathbf{r}_1(t) \\ \mathbf{r}_2(t) \\ \mathbf{r}_3(t) \end{pmatrix} .$$

The matrix is the Pascal triangle matrix and the generalization to the sixth order form is evident. The equations of motion enter through the corrector step. Evaluating the forces with $\mathbf{r}_0^p(t+\delta t)$ gives the correct second order derivative $\mathbf{r}_2^c(t+\delta t)$. The error in the prediction step is given by

$$\Delta\mathbf{r}_2(t+\delta t) = \mathbf{r}_2^c(t+\delta t) - \mathbf{r}_2^p(t+\delta t) .$$

Using this error the corrected values are

$$\begin{pmatrix} \mathbf{r}_0^c(t+\delta t) \\ \mathbf{r}_1^c(t+\delta t) \\ \mathbf{r}_2^c(t+\delta t) \\ \mathbf{r}_3^c(t+\delta t) \end{pmatrix} = \begin{pmatrix} \mathbf{r}_0^p(t+\delta t) \\ \mathbf{r}_1^p(t+\delta t) \\ \mathbf{r}_2^p(t+\delta t) \\ \mathbf{r}_3^p(t+\delta t) \end{pmatrix} + \begin{pmatrix} c_0 \\ c_1 \\ c_2 \\ c_3 \end{pmatrix} \Delta\mathbf{r}_2(t+\delta t) .$$

Gear discussed the best choice for the corrector coefficients c_i, which depends on how many derivatives of $\mathbf{r}_i$ are used (Allen and Tildesley, 1989; Gear, 1966; Gear, 1971). The predictor-corrector algorithm has advantages over the Verlet algorithm only for small timesteps, but having the velocities available is convenient for implementing the Berendsen controls.

4.2 Verlet algorithm

The Nose-Hoover temperature and pressure controls are incorporated in the equations of motion as friction coefficients in the time integration which is performed using the Verlet algorithm (Allen and Tildesley, 1989),(Verlet, 1967).

$$\begin{aligned} \mathbf{r}(t+\delta t) &= 2\mathbf{r}(t) - \mathbf{r}(t-\delta t) + \delta t^2\mathbf{a}(t) \\ \mathbf{v}(t) &= \frac{\mathbf{r}(t+\delta t) - \mathbf{r}(t-\delta t)}{2\delta t} \end{aligned} \tag{4}$$

The first step of the integration was computed with ordinary Taylor expansion:

$$\mathbf{r}(t+\delta t) = \mathbf{r}(t) + \delta t(v)(t) + \frac{1}{2}\delta t^2 \mathbf{a}(t)$$

5 Calculation of energies and forces

5.1 The Lennard-Jones potential

The Lennard-Jones pair potential is given by

$$V_{LJ}(r) = 4\varepsilon \left(\left(\frac{\sigma}{r} \right)^{12} - \left(\frac{\sigma}{r} \right)^{6} \right)$$

where r denotes the separation between the interacting particles. σ is determined by the equilibrium distance, i.e. the situation of minimum energy. It sets the length scale for this kind of interaction. ε is the depth of the potential and determines the energy scale.

Lennard-Jones type interactions are assumed for Ar-Ar and Ar-Cu. The parameters are for Ar $\sigma_{\text{Ar-Ar}} = 3.41$ Å, $\varepsilon_{\text{Ar-Ar}}/k_B = 119.8$ K (Allen and Tildesley, 1989) (Maitland, 1981) and for Cu $\sigma_{\text{Cu-Cu}} = 2.27$ Å, $\varepsilon_{\text{Cu-Cu}}/k_B = 6765.4$ K (cf. homework #2). From the mixing rules of Lorentz and Berthelot (Allen and Tildesley, 1989) one approximates the values for Ar-Cu: $\sigma_{\text{Ar-Cu}} = 2.84$ Å, $\varepsilon_{\text{Ar-Cu}}/k_B = 900.3$ K.

The potentials were evaluated numerically. In the code the energies and forces were calculated using spline interpolation.

5.2 The Embedded-Atom-Method

The more complex Cu-Cu interaction was computed in accord with the embedded atom method (EAM) (Daw and Baskes, 1983), (Daw and Baskes, 1984), (Foiles et al., 1986).

In this approach the overall electron density in a metal is assumed to be a *linear-superposition* of the contribution of each atom. It is mainly affected by the contribution of the atom of reference whence one approximates the other atoms by a *constant* term. The total energy can then be written as

$$E_{tot} = \sum_i F_i(\rho_{h,i}) + \frac{1}{2} \sum_i \sum_{j(\neq i)} \rho_{ij}(R_{ij}).$$

In this equation $F(\rho_{h,i})$ stands for the energy due to the *background* electronic density $\rho_{h,i}$ at atom i. The second term represents the Coulombic repulsion between the cores.

The electronic density $\rho_{h,i}$ is computed from the atomic densities $\rho_j^a(R_{ij})$ as follows:

$$\rho_{h,i} = \sum_{j(\neq i)} \rho_j^a(R_{ij})$$

In advance of simple pair potentials this approach allows for many body interactions.

6 The setup of the simulation

For this project we used the code PARCAS by Kai Nordlund which was modified to meet our requirements as described previously.

We encountered difficulties when we used the Nosé-Hoover thermostat and pressure control with systems where the atoms are far apart. If the distance between the particles is bigger than the cutoff radius of the potentials the forces will be necessarily zero. This causes problems in the Verlet integrator since the propagation of the positions – as it can be seen from eq. (4) – is determined exclusively by the accelerations, i.e. the forces, and independent of the velocities. Within the time constraints of this project this problem had to remain unsolved. The simulation of homogeneous nucleation was therefore performed entirely with the Gear predictor-corrector algorithm and the Berendsen thermostat.

We used a cubic box with side lengths of 70.0 Åcontaining 343 Ar and 343 Cu atoms. Periodic boundary conditions have been applied in all directions. In the beginning the atoms were arranged on a bcc lattice, i.e. the box was subdivided into 7x7x7 unit cells each holding two atoms, as can be seen on figure fig. 3. The initial velocities were set according to the Maxwell-Boltzmann distribution at 300 K.

The positions and its derivatives were integrated with a sixth order Gear predictor-corrector algorithm for approximately 10 ns of real time. The Berendsen thermostat with a coupling constant of 10 fs was applied to the Ar atoms only to hold the temperature about 300 K.

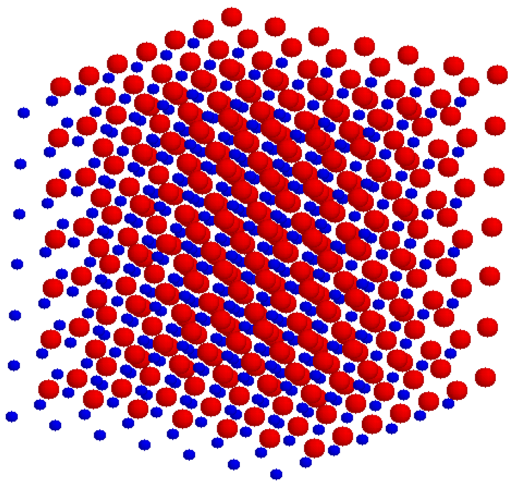

Figure 3: The setup of the simulation, Ar atoms: blue and small, Cu atoms: big and red

7 Results

During the simulations among other observables the temperature, the pressure, the kinetic and potential energy as well as the positions have been saved to disk several times. These files were used to analyze the development of the system with time where the Stillinger criterion (Ford, 1997) was used to determine if a cluster has formed.

In fig. 4 we plotted how the number of clusters, i.e. non-monomers, changes with time. One can see that the number of clusters sharply rises immediately after the simulation has been started. After that it falls continuously until it approaches one.

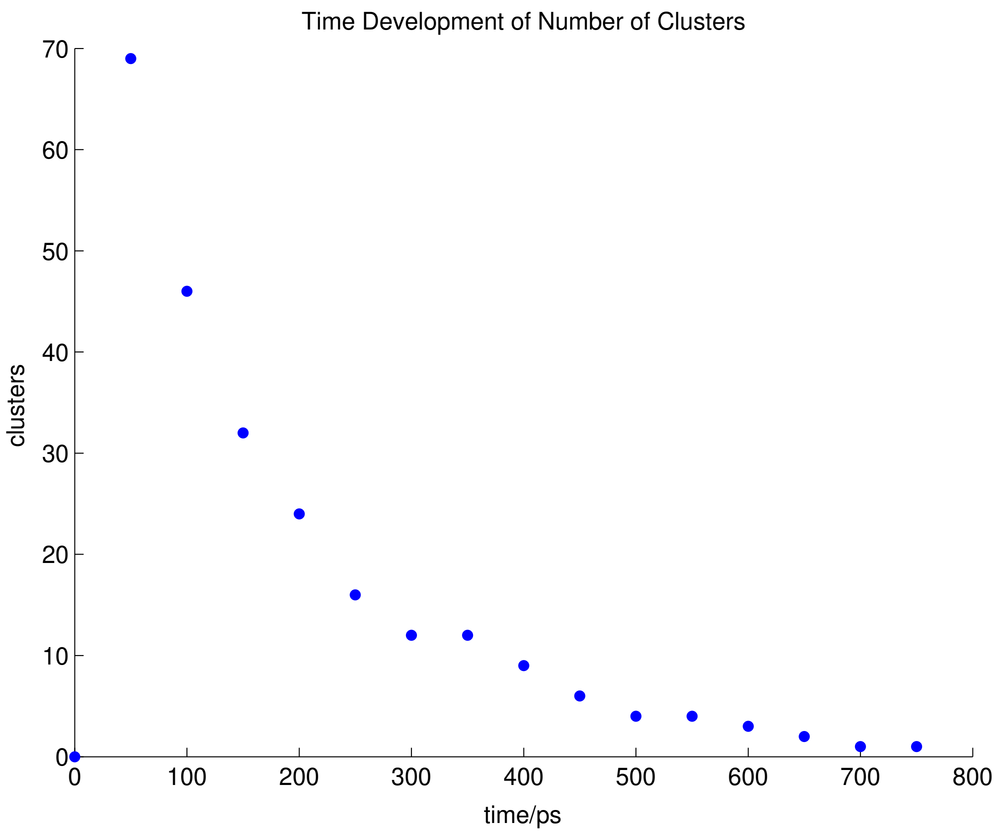

Figure 4: the number of clusters as a function of time

The free energy for the formation of a cluster $f_{cluster}$ is given by

$$\Delta f_{cluster} = f_{vap} - (f_{sol} + f_{surf})$$

where f_{vap} and f_{sol} stand for the free energy of the vapor phase and the solid state, respectively. The term f_{surf} represents the free energy of the surface which is introduced into the system. Accordingly one can explain the behavior of the system as follows: under the conditions of this simulation the vapor is no longer the most stable phase. Instead the system evolves into the solid state by forming clusters. But because in the beginning there are many small clusters the surface energy plays governing role. As time advances the smaller clusters merge to former bigger clusters and in the end only one big cluster remains. This final cluster is shown in fig. 5 and it can be seen that it has a crystalline structure.

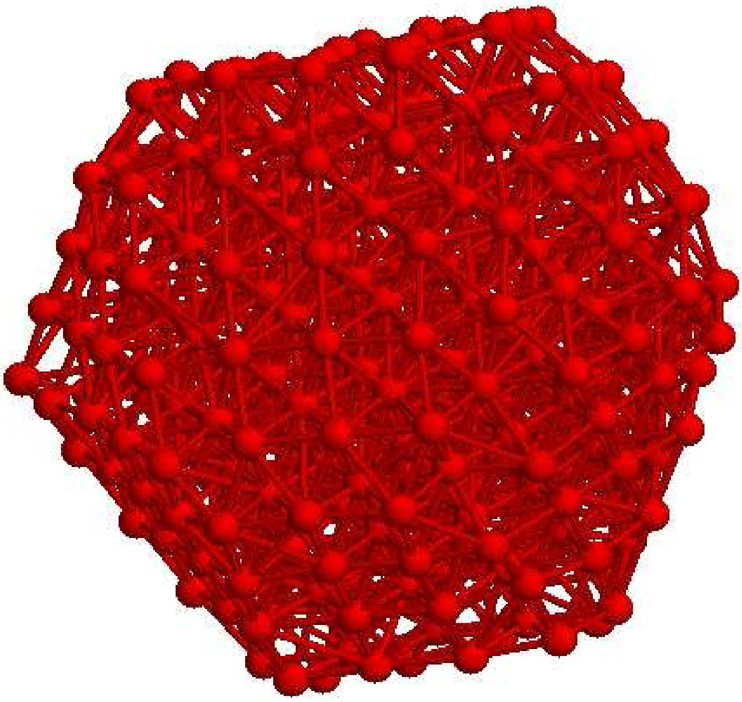

Figure 5: the cluster remaining at the end of the simulation run

As described in the preceding section only the Ar atoms are used to control the temperature of the system. Equivalent to the experiment they act as the cooling gas for the Cu atoms. The energy which is released during the formation of clusters raises the temperature of the Cu atoms; fig. 6 shows the *temperature*[1] of the Cu atoms as a function of time. It can be seen that it takes some time until the temperature is lowered due to collisions with the Ar atoms.

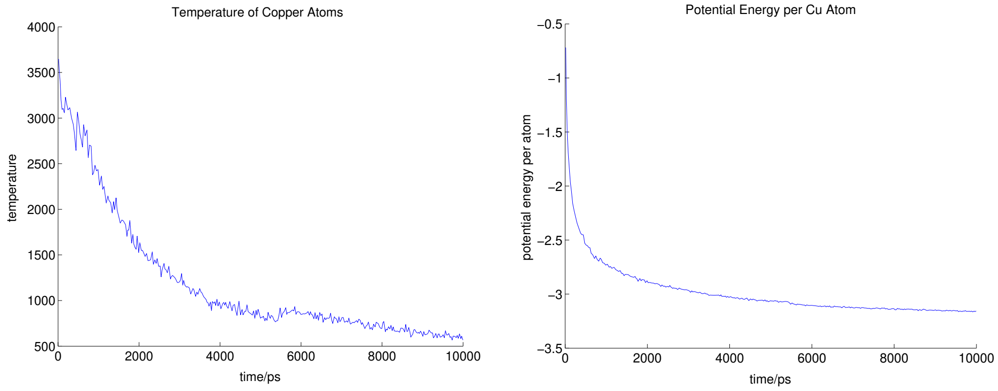

Figure 6: the temperature of the Cu atoms (cf. footnote 1) (right) and the potential energy per Cu atom as a function of time

A snapshot of the system after 100 ps is shown in fig. 7. The clustering has already begun and several bigger clusters can be identified.

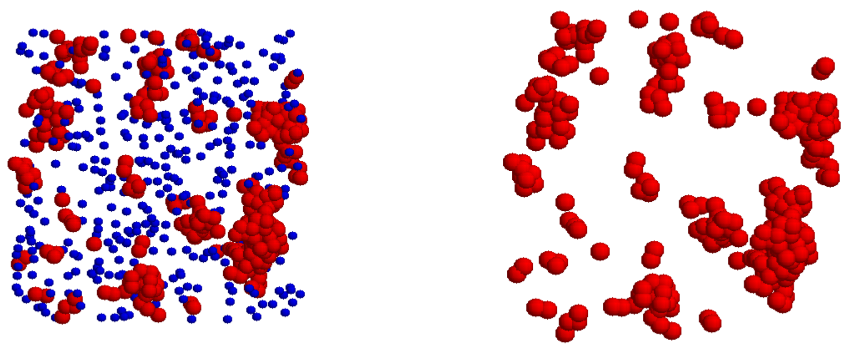

Figure 7: snapshot of the system at 100 ps, showing Ar as well as Cu atoms (left), only Cu atoms (right)

For the same instant of time the cluster size distribution and the radial distribution function have been computed (fig. 8).

[1] This hypothetical 'temperature' is computed from the kinetic energy of the Cu atoms. There is *no experimental equivalent* to this definition.

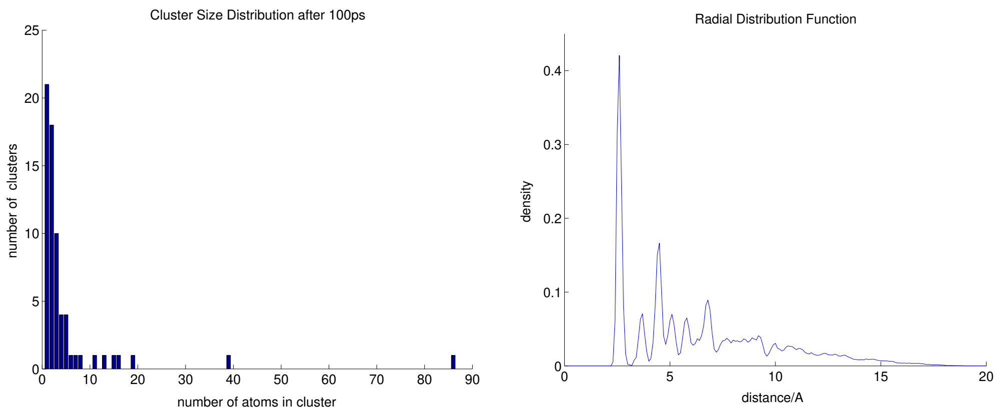

Figure 8: the cluster size distribution (left) and the radial distribution function (right) after 100 ps

8 Conclusion

We were able to reproduce the experimental behavior in the MD simulation, i.e. we observed cluster formation and growth. Unfortunately we were not able to perform the runs with the Nosé-Hoover thermostat and pressure control, yet. It would be particular interesting to study the system in the case of a true isobaric-isenthalpic (N,H,P) or isothermal-isobaric (N,T,P) ensemble. This would allow us for instance to calculate the work of expansion during cluster formation and growth. Due to constraints in time and computing power we had to restrict ourselves to a relatively small system. Especially to improve the statistics the simulation of a bigger system would be favorable.

The comparison between simulations and experiment is difficult in this case. Experiments are performed at pressures of the order 10^{-3} kbar while simulations work with pressures tens of orders bigger.

We would like to thank Robert Averback, Yinon Ashkenazy and Pavel Krasnochtchekov for their help and support.

References

Allen, M. and Tildesley, D.: 1989, *Computer Simulation of Liquids*, Oxford University Press, New York

Andersen, H.: 1980, *Journal of Chemical Physics* **72**, 2384

Berendsen, H., Postma, J., Gunsteren, W. V., Nola, A. D., and Haak, J.: 1984, *Journal of Chemical Physics* **81**, 3684

Daw, M. and Baskes, M.: 1983, *Physical Review Letters* **50(17)**, 1285

Daw, M. and Baskes, M.: 1984, *Physical Review B* **29(13)**, 6443

Foiles, S., Baskes, M., and Daw, M.: 1986, *Physical Review B* **33(12)**, 7983

Ford, I.: 1997, *Physicall Review E* **56(5)**, 5615

Gear, C.: 1966, *The numerical integration of ordinary differential equations of various orders*, Technical Report 7126, Argonne National Laboratory

Gear, C.: 1971, *Numerical initial value problems in ordinary differential equations*, Prentice-Hall, Englewood Cliffs, NJ

Holian, B. L., Groot, A. J. D., Hoover, W. G., and Hoover, C. G.: 1990, *Physical Review A* **41(8)**, 4552

Hoover, W. G.: 1985, *Physical Review A* **31(3)**, 1695

Hoover, W. G.: 1986, *Physical Review A* **34(3)**, 2499

Nosé, S.: 1984, *Molecular Physics* **52(2)**, 255

Nosé, S. and Klein, M.: 1983, *Molecular Physics* **50(5)**, 1055

Parrinello, M. and Rahman, A.: 1980, *Physical Review Letters*

Posch, H. A., Hoover, W. G., and Veseley, F. J.: 1986, *Physical Review A* **33(6)**, 4253

Verlet, L.: 1967, *Physical Review* **159**, 98